Journal of Engineering Physics and Thermophysics, Vol. 76, No. 4, 2003

HOMOGENEOUS NUCLEATION AND THE HEAT-PIPE BOILING LIMITATION

D. Mishkinis and J. M. Ochterbeck

UDC 536.24

Criteria for phase change in classical heat pipes and loop heat pipes with microporous capillary structures of wicks have been formulated and developed. The criteria are based on homogeneous nucleation and cluster theory to evaluate the superheat required for phase change to occur in microchannels. The results can be employed in analyzing the limiting operational criteria and heat-transfer capacity of heat pipes based on the boiling limit.

Two key phrases are widely used in boiling phenomena theory and practice for heat-pipe applications. The first is general and fundamental: "To boil or not to boil ..." [1]. The second is specific for loop heat pipes and belongs to Mr. David Antoniuk of the TRW Space & Technology Division (U.S.): "No bubble – no trouble!" Both phrases highlight the need for predictive theories in terms of when bubble generation will occur.

Numerous books and papers have been dedicated to boiling and evaporation processes in heat pipes, but this problem still has a lot of obscurities. In the "classical" heat-pipe literature (see, for instance, [2, 3]) the parameter "nucleation radius of the vapor bubbles, r_n" is introduced for boiling limitation calculation. This parameter should be determined from specific and complicated experiments for every capillary structure, heat pipe enclosure, and working liquid. Peterson [2] and Chi [4] (with reference to [5]) suggest using, for estimation of the boiling limitation, values within the range 10^{-5}–10^{-3} in [$2.54\cdot(10^{-7}$–$10^{-5})$ m]. This range is very wide. In practice, this leads us to conclude that the calculation of the boiling limitation according to "classical" models is of no practical importance for microporous capillary wicks when the effective pore size is of the same order as the nucleation site. Also, the majority of researchers suppose *a priori* that boiling in such heat pipes will never be realized because the wick drying due to the capillary limitation will occur first. Microporous capillary wicks are the central element of the new generation of heat pipes, i.e., loop heat pipes (LHP). LHPs have specific features when compared to standard heat pipes: separated liquid and vapor channels and specially designed evaporators. The wick (capillary pump that promotes liquid circulation during LHP operation) is placed only in the evaporator; a schematic of a typical evaporator is presented in Fig. 1. The wick capillary structure is modeled as a bundle of cylindrical parallel capillaries with fixed diameter, which is equal to the effective pore diameter.

The following example for an ammonia LHP evaporator (operational temperature T_v = 20°C, wick material nickel, inner wick diameter D_1 = 16 mm, outer wick diameter D_2 = 24 mm, evaporator length L = 100 mm, porosity ε = 70%, effective thermal conductivity of the wick λ_s = 7 W/(m·K)) with different effective pore radii of the wick r = 1–50 μm is used for illustration of the impossibility of using classical heat-pipe boiling limitation theory in the case of microporous wicks. The classical equations for boiling critical superheat and for boiling heat-transfer limit [5] are

$$\Delta T_{sh} = \frac{2\sigma T_v}{h_{fg}\,\rho_v}\left(\frac{1}{r_n} - \frac{1}{r_p}\right), \tag{1}$$

$$Q_{b\,max} = \frac{4\pi\sigma L \lambda_{eff} T_v}{h_{fg}\,\rho_v \ln\,(D_1/D_2)}\left(\frac{1}{r_n} - \frac{1}{r_p}\right). \tag{2}$$

Results of the calculations are presented in Fig. 2. Even insignificant changes of the effective radius r_n lead to serious change of the temperature superheat and heat transfer. Moreover, according to this model, the given ammonia heat pipe is incapable of transfering more than 20–25 W (0.27–0.33 W/cm^2) due to boiling limitation. But, in

Clemson University, Clemson, SC 29631; email: Donatas@CLEMSON.EDU. Published in Inzhenerno-Fizicheskii Zhurnal, Vol. 76, No. 4, pp. 61–64, July–August, 2003. Original article submitted December 24, 2002.

1062-0125/03/7604-0813$25.00

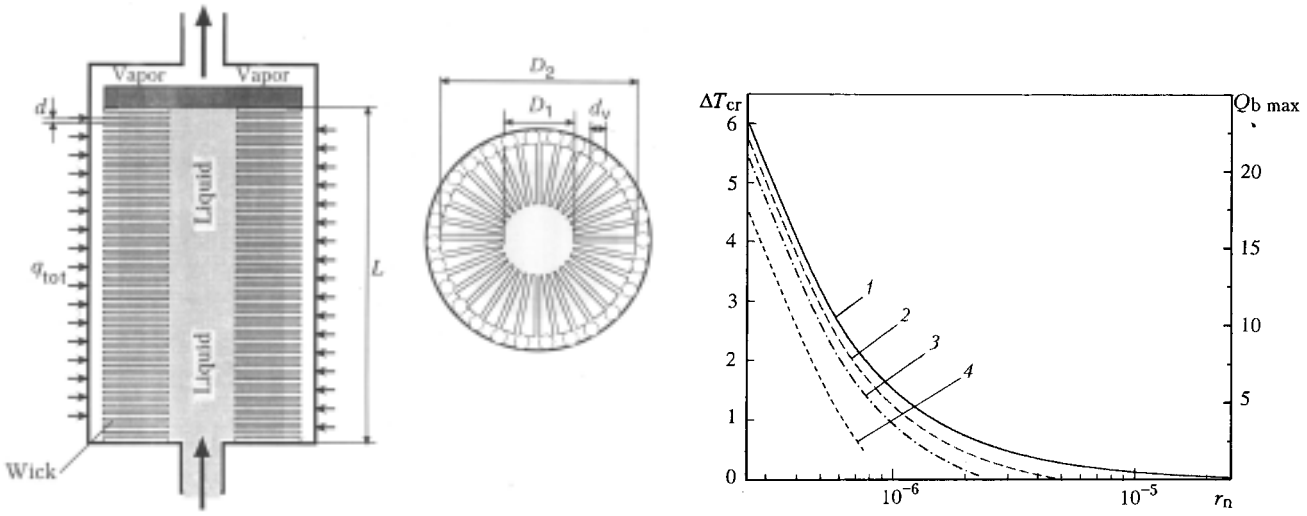

Fig. 1. Schematic of an LHP evaporator.

Fig. 2. Critical heat transfer and superheat temperature drop vs. nucleation site radius for different wick effective pore radii (ammonia LHP with a nickel wick): 1) r = 50; 2) 5; 3) 2.5; 4) 1 μm. ΔT_{cr}, K; $Q_{b\ max}$, W; r_n, *m*.

practice, loop heat pipes with similar parameters can transfer up to several hundred watts. This model is based on the suggestion that the nucleation centers are microscopic cavities with entrapped noncondensed gases, which are placed in the gap between the capillary wick and the heat-pipe envelope. The presence of such cavities results in boiling phenomenon at very small superheat levels (within a few degrees relative to the working-liquid saturation temperature). If the whole of the noncondensable gas was preliminarily removed from the system, the liquid superheat could reach up to 100–200 K before boiling was started. This was experimentally confirmed by Harvey and co-workers in the 1940's in [6], where surface cavities were deactivated by subjecting the tested liquid and surface to high static pressures before the boiling point at atmospheric pressure measurements. The preliminarily pressurized samples boiled at very high temperatures close to the superheat limit. So, in the experiments the authors dealt with pure liquids and pure surfaces without dissolved gases in the system. Heat-pipe manufacturers always strive toward minimization of the noncondensable-gas volume inside the heat pipe or toward a lower amount of noncondensable gas there for more predictable and reliable operation of the heat pipe. Thus, the better the heat pipe, the less the probability of reaching its boiling limitation. Another example that confirms this conclusion is the experimental work of R. R. Barthelemy [7], who focused special attention on the liquid degassing (20 min boiling of demineralized, triply deionized, and triply distilled water just before filling) and on noncondensable gas evacuation (10^{-5} Torr) from the heat-pipe enclosure before filling. Bubble boiling was not observed in heat pipes with good contact of the capillary wick with the pipe wall. However, if this contact was poor, vapor bubble generation was observed in the regions of poor contact. This can be explained by the presence of microcavities at the pipe wall, which were filled by noncondensable gas. The gas molecules inside cavities were in the adsorbed state and were also trapped there by water from the heat-pipe volume during the filling process. When contact between the wick and wall was better, a smaller number of cavities were possible as nucleation centers and the highest superheat levels could be achieved. Another possible reason for boiling in heat pipes with gaps between the envelope and wick is the small nucleus formation time for the gap in comparison to the wick pores ($V_{gap} >> V_{pore}$):

$$t_{nc\ gap} \sim (J_{nc} V_{gap})^{-1} << t_{nc\ pore} \sim (J_{nc} V_{pore})^{-1}.$$

Additionally, liquid in the gap can be stagnant but the liquid in the evaporator wick pores is always replaced during heat-pipe operation by returning flow from the condenser. One of the principal conclusions of Barthelemy is that nucleation boiling is not an important mechanism in a well-fabricated heat pipe. It is justified for heat pipes that operate in temperature regions far from the critical temperature of the working liquid (for instance, water heat pipes in

TABLE 1. Ammonia Boiling Parameters

T_v, °C	r_p, μm	$J_{nc\ hp}$, $(m^3 \cdot sec)^{-1}$	n_{cr}	$T_{sh} - T_v$, °C	T_{sh}/T_{cr}	$Q^*_{b\ max}$, W	$q_{b\ max}$, W/cm^2
$q = 1$ W/cm^2							
20	1	$2.78 \cdot 10^{11}$	2789	74.7	0.91	283.4	3.8
	2.5	$4.45 \cdot 10^{10}$	2902	74.3	0.91	281.9	3.7
	5	$1.11 \cdot 10^{10}$	2990	74.1	0.91	281.2	3.7
	50	$1.11 \cdot 10^{8}$	3281	73.3	0.90	278.1	3.7
40	1	$2.78 \cdot 10^{11}$	2991	57.7	0.92	215.4	2.9
	2.5	$4.45 \cdot 10^{10}$	3113	57.4	0.92	214.3	2.8
	5	$1.11 \cdot 10^{10}$	3206	57.2	0.92	213.6	2.8
	50	$1.11 \cdot 10^{8}$	3520	56.4	0.91	210.6	2.8
60	1	$2.78 \cdot 10^{11}$	3345	42.2	0.93	155.1	2.1
	2.5	$4.45 \cdot 10^{10}$	3482	41.9	0.93	154.0	2.0
	5	$1.11 \cdot 10^{10}$	3587	41.7	0.93	153.3	2.0
	50	$1.11 \cdot 10^{8}$	3941	41.1	0.92	151.0	2.0
$q = 10$ W/cm^2							
20	1	$2.78 \cdot 10^{12}$	2648	75.1	0.91	285.0	3.8
	2.5	$4.45 \cdot 10^{11}$	2760	74.7	0.91	283.4	3.8
	5	$1.11 \cdot 10^{11}$	2846	74.5	0.91	282.7	3.8
	50	$1.11 \cdot 10^{9}$	3134	73.7	0.90	279.7	3.7
40	1	$2.78 \cdot 10^{12}$	2839	58.1	0.92	216.9	2.9
	2.5	$4.45 \cdot 10^{11}$	2960	57.8	0.92	215.8	2.9
	5	$1.11 \cdot 10^{11}$	3052	57.5	0.92	214.7	2.9
	50	$1.11 \cdot 10^{9}$	3363	56.8	0.91	212.1	2.8
60	1	$2.78 \cdot 10^{12}$	3174	42.5	0.93	156.2	2.1
	2.5	$4.45 \cdot 10^{11}$	3310	42.2	0.93	155.1	2.1
	5	$1.11 \cdot 10^{11}$	3413	42.0	0.93	154.4	2.1
	50	$1.11 \cdot 10^{9}$	3762	41.4	0.92	152.2	2.0

the Barthelemy experiments). As a confirmation of this conclusion, we can also refer to experiments with boiling nucleation in microscale channels conducted by X. F. Peng et al. [8]. The liquid superheat temperature in these experiments was of the same order as that for homogeneous nucleation in an unconstrained liquid. Every pure liquid has a highest attainable temperature for which nucleation will not occur, i.e., a superheat limit or explosion temperature (for given pressure conditions). This temperature is closely connected with the concept of liquid tensile strength. As a rule, the superheat temperature for liquid boiling at atmospheric pressure is in the range $(0.8–0.95)T_{cr}$ [6, p. 91]. In this case, the vapor bubble formation is connected with a molecular cluster appearance in the liquid, and this process is described by kinetic theory.

Today, there are two main approaches to theoretical calculation of the liquid superheat limit: the "classical" [6, pp. 75–79] and the model developed by H. Y. Kwak et al. [9, 10]. The difference lies in understanding of the surface energy of clusters. In the classical model, the value of the liquid surface tension, an equilibrium property of the macroscopic interface, is used. In the Kwak model, surface energy for vapor bubble formation is assigned as the energy required to cut across a cluster composed of activated molecules. Both models can predict superheat limit with high accuracy. But the Kwak model looks physically more realistic and, moreover, this method allows predicting the decompression level for bubble formation in liquid–gas solutions and the tensile strength of liquids (in this case, classical theory fails). That is why the Kwak model was chosen for superheat-limit calculations. This temperature does not depend on any outside introduced parameters, such as the radius of the nucleation site, but depends only on the physical properties of the liquid and the operational temperature of the heat pipe (vapor temperature). Superheating depends

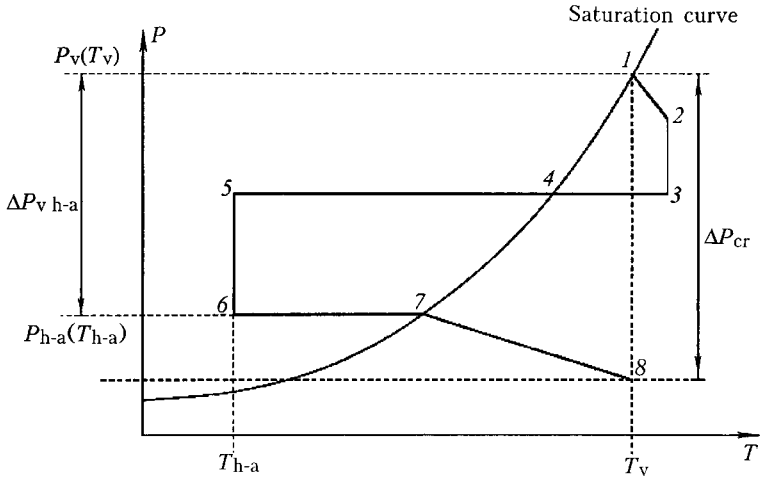

Fig. 3. The pressure–temperature diagram of an LHP operation [13].

on the wick properties indirectly, not directly as in Eq. (1). One of the unknown parameters for superheat determination is the nucleation rate J_{nc}. The value $J_{nc} = 10^6$ nuclei/(m^3·sec) is considered to be the threshold of bubble formation, and $J_{nc} = 10^{12}$ nuclei/(m^3·sec) correspond to the massive bubble formation according to "classical" superheat limit theory. But in practice, the nucleation rate for vapor explosion can reach values up to $J_{nc} = 10^{28}$ nuclei/(m^3·sec) [10].

For heat pipes this threshold nucleation rate can be estimated from the following discourse. If the applied heat rate q is known, we can estimate the time of liquid replacement in the evaporator zone, and because the nucleus formation time is $[J_{nc}\pi r^2(D_1 - D_2)/2]^{-1}$(the wick is modeled as a series (bundle) of independent parallel cylindrical channels), we have

$$J_{nc\ hp} = \frac{q}{h_{fg}\,\rho_{liq}\pi\,(r_p\,(D_1 - D_2)/2)^2}\,. \tag{3}$$

After calculation of the superheat limit temperature T_{sh} from the Kwak model and Eq. (3), we can estimate the critical boiling heat transfer:

$$Q^*_{b\ max} = \frac{2\pi L\lambda_{eff}}{\ln\,(D_1/D_2)}\,(T_{sh} - T_v)\,. \tag{4}$$

The results of modeling (for applied heat rates q = 1 and 10 W/cm^2) are presented in Table 1, where n_{cr} is the number of molecules in the critical cluster. If a critical cluster, corresponding to the given conditions, is formed, its growth to a macroscopic vapor bubble is guaranteed.

The dependence of the effective pore radius on the critical boiling heat transfer is weak. But, when the operation temperature of the heat pipe is closer to the critical region, it is more important to take into account the explosive boiling phenomenon. From Table 1 it is seen that the heat pipe with applied heat load of 10 W/cm^2 will not function at the given operational temperatures due to reaching the boiling limitation. The following estimation methods for the temperature dependence of the ammonia properties were used in [11]: Carruth–Kobayashi for enthalpy of vaporization, Gunn–Yamada for liquid density, and Lee–Kesler for pressure. The Kwak method of superheat temperature calculation is shown in the Appendix.

Equation (4) is equitable for ordinary heat pipes when the heat load is applied to the heat-pipe enclosure and transferred through the liquid-saturated wick to the liquid/vapor phase boundary by conduction. The maximum superheated liquid in this case is placed in the region next to the heat-pipe enclosure wall. Another situation is realized in LHPs and capillary pumped loops (CPLs). The phase boundary in this case is placed inside the capillary wick and the distance between the boundary and evaporator enclosure wall is filled by saturated and overheated vapor. It should be mentioned that if the LHP/CPL evaporator is designed in a such way that contact between the evaporator wall and the liquid agent is eliminated during LHP/CPL operation, then the presence of gas-filled microcavities at the evaporator

wall does not have any influence on boiling initiation in the heat pipe. Thus, if the purity of the working fluid is high, the explosive boiling in the evaporator will start only when the superheat limit conditions for liquid in the capillary wick are reached. From a thermohydraulic analysis of LHP operation [12], it follows that the maximum superheated liquid is placed just under the evaporating inverted meniscus. An analogous thermohydraulic analysis was made by Yu. F. Maidanik et al. [13]. The pressure–temperature diagram of LHP operation is presented in Fig. 3. According to this diagram, the operational condition of an LHP as a capillary-pumped device can be presented in the traditional manner:

$$\Delta P_{\text{cap max}} = \frac{2\sigma}{r_{\text{p}}} \geq \Delta P_{\text{cap}} = \Delta P_{\text{LHP}} \approx \frac{2\sigma \cos\theta}{r_{\text{p}}}, \tag{5}$$

where ΔP_{cap} is the capillary head, ΔP_{LHP} is the total pressure losses along the circulation loop (including losses in vapor grooves 1–2, vapor line 2–3, liquid line 5–6, and wick 7–8), and θ is meniscus apparent contact angle in the wick. Thus, the explosive boiling condition and the boiling limit condition in an LHP are the following:

$$T_{\text{v}} = T_{\text{sh}}\left(P_{\text{v}}\left(T_{\text{v}}\right) - \Delta P_{\text{cap}}\right), \tag{6}$$

$$\frac{T_{\text{v}}}{T_{\text{sh}}\left(P_{\text{v}}\left(T_{\text{v}}\right) - \Delta P_{\text{cap}}\right)} \leq 1. \tag{7}$$

It is very difficult to reach this limitation because ΔP_{cap}, as a rule, is of the order of 1 bar or less and $P_{\text{v}}(T_{\text{v}}) - \Delta P_{\text{cap}} \approx P_{\text{v}}(T_{\text{v}})$ is in the liquid critical region. This leads to the conclusion that if the LHP/CPL is fabricated and filled by a working agent with a high degree of carefulness and thoroughness that eliminate the presence of non-condensable gases (adsorbed, absorbed, and dissolved) in the system, practically no boiling phenomenon will be realized during LHP operation. It should be mentioned that we are not talking about LHP start-up conditions or regions outside of the wick structure. These problems must be considered separately. Preliminary high static pressurization of the heat-pipe envelope (evaporator for the LHP) filled by the working liquid can be recommended as one of the stages of the heat-pipe manufacturing process.

APPENDIX

Kwak Model for Superheat Temperature Calculation

First, $J_{\text{nc hp}}$ from Eq. (3) is calculated. Then the initial data for ammonia are introduced:

P_{∞}, pressure of saturated vapor at operational temperature;

ρ_{cr} = 225 kg/m^3 and T_{cr} = 405.35 K, ammonia critical density and temperature;

$d_{\text{W}} = 2.9\cdot10^{-10}$ m, Van der Waals diameter of an ammonia molecule;

$E_{\text{i}} = 1.6454\cdot10^{-18}$ J, ammonia ionization potential;

$\alpha = 2.39\cdot10^{-30}$ m^3, ammonia polarizability;

T_{F} = 195.42 K, fusion temperature;

ΔH_{F} = 332941.176 J, enthalpy of fusion;

m = 17, molar mass;

z = 12, coordination number for FCC lattice;

β = 1, accommodation coefficient;

$\varepsilon_0 = \dfrac{3E_{\text{i}}\alpha^2}{16d_{\text{W}}^6}$, Lennard-Jones potential parameter;

$T_{\text{sh}\,0} = 0.75T_{\text{cr}}$, initial value of superheat temperature.

From this point the iteration cycle for T_{sh} is started. The following parameters corresponding to $T_{\text{sh}\,0}$ are calculated:

h_{fg}, enthalpy of vaporization;

ρ_{liq}, density of liquid; N = Na ρ_m/m;

$d_m = \left(\dfrac{6 \cdot 0.7405}{\pi N}\right)^{1/3}$ and $V_m = \dfrac{\pi d_m^3}{6}$, average distance between molecules in the liquid and effective molecular volume of the liquid;

$\varepsilon_m = 4\varepsilon_0 \left[1 - \left(\dfrac{\rho_{cr}}{\rho_{liq}}\right)^2\right] \left[\left(\dfrac{d_W}{d_m}\right)^6 - \left(\dfrac{d_W}{d_m}\right)^{12}\right]$, energy required to separate a pair of molecules from d_m to the mean distance between molecules at the critical point;

$D_e = \beta N \left(\dfrac{8kT_s}{\pi m}\right)^{1/2} \exp\left(-\dfrac{h_{fg}}{RT_{sh\,0}} - \dfrac{\Delta H_f}{RT_f}\right) \pi \left(\dfrac{3V_m}{4\pi}\right)^{2/3}$, coefficient;

$Z_f = \left(\dfrac{z\varepsilon_m}{18\pi k T_s}\right)^{1/2}$, Zel'dovich nonequilibrium factor;

$n_{cr} = \left[\dfrac{6kT_s}{z\varepsilon_m} \ln\left(\dfrac{J_{nc\,hp}}{N D_e Z_f}\right)\right]^{3/2}$, number of molecules in the critical cluster;

$P_v = \left(\dfrac{z\varepsilon_m}{3}/V_m\right) \Big/ n_{cr}^{1/3} + P_\infty$, vapor pressure.

Now we determine the temperature $T_{sh\,1}$ (which corresponds to the obtained P_v). If $|T_{sh\,0} - T_{sh\,1}| > 0.05$, $T_{sh\,0} = T_{sh\,1} + 0.005$ and the cycle is repeated. Thus, finally $T_{sh} = T_{sh\,x}$. This is the superheat limit.

NOTATION

d, diameter; D_1, inner wick diameter; D_2, outer wick diameter; J_{nc}, nucleation rate; h_{fg}, latent heat of evaporation; k, Boltzmann constant; L, length of evaporator active zone; Na, Avogadro number; N, number density; n_{cr}, number of molecules in the critical cluster; P, pressure; Q, heat transfer; q, heat rate; r, radius; R, gas constant; r_n, nucleation radius of the vapor bubbles; T, temperature; t, time; t_{nc}, nucleus formation time; V, volume; ρ density; ε, porosity; λ, thermal conductivity; σ, surface tension; θ, contact angle. Subscripts: cr, critical; b, boiling; v, vapor; liq, liquid; eff, effective; p, wick pore; cap, capillary; sh, superheat; hp, heat pipe; max, maximum; s, solid; h-a, hydro-accumulator; LHP, loop heat pipe.

REFERENCES

1. I. R. Martin-Dominguez and T. W. McDonald, *ASHRAE Trans.*, **103**, No. 1, 348–355 (1997).
2. G. P. Peterson, *An Introduction to Heat Pipes: Modeling, Testing, and Applications*, Wiley, New York (1994).
3. P. D. Dunn and D. A. Reay, *Heat Pipes*, 3rd edn., Pergamon, New York (1982).
4. S. W. Chi, *Heat Pipe Theory and Practice*, McGraw-Hill, New York (1976).
5. B. D. Marcus, *Theory and Design: Variable Conductance Heat Pipes*, NASA CR-2078, Washington, DC (1972).
6. S. V. Stralen and R. Cole, in: *Boiling Phenomena: Physicochemical and Engineering Fundamentals and Applications*, Vol. 1, Hemisphere (1979), pp. 119–121.
7. R. R. Barthelemy, in: *Proc. 2nd Int. Heat Pipe Conf.*, Bologna (1976), pp. 425–437.
8. X. F. Peng, G. P. Peterson, and B. X. Wang, *Exp. Heat Transfer*, **7**, No. 4, 249–264 (1994).
9. H. Y. Kwak and R. L. Panton, *J. Phys. D: Appl. Phys.*, **18**, 647–659 (1985).
10. H. Y. Kwak and S. Lee, *Trans. ASME, J. Heat Transfer*, **113**, 714–721 (1991).
11. R. C. Reid, J. J. Prausnitz, and T. K. Sherwood, *The Properties of Gases and Liquids*, 3rd edn., McGraw-Hill, New York (1976).
12. Jentung Ku, *Operational Characteristics of Loop Heat Pipes*, SAE Paper 1999-01-2007 (1998).
13. Yu. F. Maidanik and Yu. G. Fershtater, in: *Proc. 10th Int. Heat Pipe Conf.*, Stuttgart (1997), Paper No. X-7.